A new method to dynamically simulate groundwater table in land surface model VIC*

YANG Hongwei** and XIE Zhenghui

(LASG, Institute of Atmospheric Physics, Chinese Academy of Sciences, Beijing 100029, China)

Received April 1, 2003; revised May 20, 2003

Abstract Soil moisture plays an important role in water and energy balance in land-atmospheric interaction, but is impacted directly by the groundwater table. Dynamic variation of the groundwater table can be described mathematically by a moving boundary problem. In this paper, the moving boundary problem is reduced to a fixed boundary problem through a coordinate transformation. A new model of groundwater table simulation is developed using the mass-lumped finite element method and is coupled with the land surface model of Variable Infiltration Capacity (VIC). The simulation results show that the new model not only can simulate the groundwater table dynamically, but also can evade the choice of water table depth scale in computation with a low computation cost.

Keywords: land-atmospheric interactions, groundwater table, VIC model.

China is a developing country with the largest population in the world. China's energy resourses per person and water resources per person are only one half and a quarter of the world average, respectively. Although the climate of the inland river areas in the north is continental, the climates of the other zones are continental monsoon climates. The distribution of regional precipitation per year is not even. Totally, the precipitation per person is five percent of the world average[1]. The semi-arid region and semi-humid region are the main production areas of wheat and cotton in China, but the peak period of water use in agriculture is just the low water season every year, so the climate is unfavorable to crop growth. Before the 1940s or 1950s, the level of productivity was very low, so the water resources were not short. In fact, like other resources, water also has an inherent regeneration period and there is a limitation on maximum exploitation. Many developed countries have adopted measures to prevent water resources from being over exploited, such as America and Japan. But currently in China, excessive exploitation of groundwater usually occurs. The impact of climate change on water resources is arousing people's interest. However, in the continental scale of China, the problem of land-atmospheric interactions is not being researched systematically, and especially the understanding of how long the changes in water resources will affect the environment is very insufficient. Many studies indicate that global temperature will increase by 3 ℃ or 4 ℃ in 100 years. This will accelerate the water cycle and make the probability and the intensity of extreme precipitation increase. At the same time, the sea level will rise and sea water inbreak will be pricked up.

Water balance is an important component of the land surface process. After precipitation reaches the surface of the ground, some of it infiltrates into the soil becoming soil moisture or ground water, and some of it flows into rivers or lakes becoming land surface water. Ground water and surface water converge to the sea mainly via rivers. A lot of surface water, soil moisture, and ground water return to atmosphere through evapotranspiration, and some will precipitate to the Earth's surface again. As the depth to the surface of the groundwater is shallow, the groundwater table distribution is therefore closely related with soil moisture. The interaction between them is an important physical process of land-atmospheric interactions[2~6]. In the coupling of a regional or global climate model with a land surface model, the latter supplies the former's lower boundary conditions. Impact of the groundwater level on the soil moisture, and further, the water and energy budgets in the climate model is more important[3~10]. Most of

* Supported by the Major State Basic Research Development Program of China (Grant Nos. G1998040905 and 2001CB309404), the National Natural Science Foundation of China (Grant Nos. 40275023 and 40145020), the Hundred Talents Program of the Chinese Academy of Sciences, and the Knowledge Innovation Project of the Institute of Atmospheric Physics of the Chinese Academy of Sciences

** To whom correspondence should be addressed. E-mail: hyang@lasg.iap.ac.cn

land surface models, such as IAP94[3], VIC[4,5,11,12], BATS, LSM, SIB[10], consider the variation of soil moisture only near the land surface, and suppose that the lower boundary condition of the soil moisture process is a constant or merely due to gravitational drainage. By neglecting the dynamic variability of the groundwater table, the mechanism of soil moisture flow is unreasonable, which brings a disadvantage to the simulation and prediction research. Recently, Xie et al. transformed the dynamic presentation of the groundwater table in the land surface model into a moving boundary (between saturated and unsaturated flow) problem, and the mass-lumped finite element method was introduced to establish the numerical model. The soil moisture model was coupled with the VIC model so it could present the groundwater table dynamically in land-atmospheric interactions. In their method, the saturated and unsaturated areas are delaminated uniformly, and the Richards equation is solved with the pre-estimate and correct iteration processes.

In this paper, a coordinate transform is used to reduce the moving boundary problem to a fixed boundary problem[13]. Discretization is considered only in the unsaturated area and thus with the same number of discrete layers, the grid resolution is raised. During the solving step, the grid number is fixed, and with about 20 grid points, a high resolution result can be obtained, so the computational cost is decreased. The results given by the new soil moisture model coupled with the VIC model show that not only can the new method simulate the groundwater table dynamically, but also the choice of water table depth scale is avoided and the computational cost is decreased. The coupled model can be applied to the simulations of land-atmospheric interaction, climate, and water resources.

1 Parameterization of a groundwater table in a land surface model

Soil moisture can be in the forms of vapourous water, adsorption water, capillary water, and gravitational water. The gravitational water moves downward and gathers above the impermeable layer. Thus the porosity of this layer is filled by soil moisture, so the layer is named the saturated zone. Except for adsorption water and capillary water, most of the porosity above the saturated zone is filled with air and so this layer is named the vadose zone. The interface between the saturated zone and vadose zone is the groundwater table. The pressure at the groundwater table is the atmospheric pressure.

Based on the horizontal resolution of the general circulation model, the horizontal movement of soil moisure is neglected. Considering the saturated and unsaturated water flow problems in one dimension, let the z axis downward be positive and the origin of the coordinate be the land surface. $\tilde{\theta}(z,t)$ is the volumetric moisture content at time t and depth z. Under the condition of nonconstant infiltration or evaporation on the land surface, let the infiltration be positive and the evaporation be negative. Based on the Darcy's law and the principle of continuity, we obtain the following Richards equation of the unsaturated flow:

$$\frac{\partial\tilde{\theta}}{\partial t}=\frac{\partial}{\partial z}\left(D(\tilde{\theta})\frac{\partial\tilde{\theta}}{\partial z}\right)-\frac{\partial K(\tilde{\theta})}{\partial z},\qquad(1)$$

where $\tilde{\theta}[L^3/L^3]$ is the volumetric moisture content, $D(\tilde{\theta})[L^2/T]$ the soil water diffusivity, and $K(\tilde{\theta})[L/T]$ the unsaturated hydraulic conductivity. The upper boundary condition can be written as

$$q_0(t)=K(\tilde{\theta})-D(\tilde{\theta})\frac{\partial\tilde{\theta}}{\partial z},\qquad(2)$$

where $q_0(t)$ is the flux of the land surface (infiltration or evaporation). In most land surface models, the following fitting relations are taken[14]:

$$K(\tilde{\theta})=K_s\left(\frac{\tilde{\theta}}{\theta_s}\right)^{2b+3},$$

$$D(\tilde{\theta})=-\frac{bK_s\Psi_s}{\theta_s}\left(\frac{\tilde{\theta}}{\theta_s}\right)^{b+2},$$

where K_s is the saturated hydraulic conductivity, θ_s the saturated volumetric moisture content, Ψ_s the saturated water head, and b the Clapp and Hornberger constant[15].

Let $\alpha(t)$ be the depth from the land surface to the groundwater table. The groundwater table (moving boundary) divides the saturated and unsaturated areas into two different parts. So, at the groundwater table, we have

$$\tilde{\theta}(z,t)=\theta_s.\qquad(3)$$

A zero pressure condition and given flux condition at the groundwater table are usually used to describe the moving boundary. In this paper, the latter is chosen. We suppose that

$$\left[K(\tilde{\theta})-D(\tilde{\theta})\frac{\partial\tilde{\theta}}{\partial z}\right]\bigg|_{z=\alpha(t)}-Q_b(t)=-n_e\frac{d\alpha}{dt},\qquad(4)$$

where $Q_b(t)$ is the base flow[4], and n_e the effective porosity in the porous medium[16]. The initial condition is

$$\tilde{\theta}(z,0) = \tilde{\theta}_0(z), \quad 0 \leqslant z \leqslant \alpha(0), \tag{5}$$

and at $z = \alpha(0)$

$$\tilde{\theta}_0(z) = \theta_s. \tag{6}$$

The soil moisture distribution $\tilde{\theta}(z, t)$ and the groundwater table $\alpha(t)$ are solved by (1) and (4) with the boundary conditions (2) and (3) and the initial conditions (5) and (6). The evaporation from the top layer (a 10 cm soil layer from the land surface in the VIC model), the transpiration from vegetation roots, and the base flow from the unsaturated area are presented in (2) and (4). If the groundwater table $\alpha(t)$ is known, the soil moisture of the unsaturated area can be obtained with the common numerical methods (see Refs. [17~19]). In this study, $\alpha(t)$ is time dependent. Supposing that

$$\bar{\tilde{\theta}}(t) = \int_0^{\alpha(t)} \tilde{\theta}(z,t)\mathrm{d}z,$$

integrating (1) on the interval $(0, \alpha(t))$, and considering (2) and (4), we can get $\frac{\mathrm{d}\bar{\tilde{\theta}}}{\mathrm{d}t} - \frac{\mathrm{d}\alpha}{\mathrm{d}t}(\theta_s + n_e) = q_0(t) - Q_b(t)$. Let $x = \frac{z}{\alpha(t)}$, $\tau = t$. Then the primitive equation can be rewritten as

$$\theta_\tau + \left(\frac{(2b+3)K_s}{\alpha\theta_s^{2b+3}}\theta^{2b+2} - \frac{x}{\alpha}\dot{\alpha}\right)\theta_x = -\frac{bK_s\Psi_s}{\alpha^2(b+3)\theta_s^{b+3}}(\theta^{b+3})_{xx}, \tag{7}$$

and correspondingly, the upper and lower boundary conditions are $q_0(\tau) = K(\theta) - \frac{D(\theta)}{\alpha}\theta_x\Big|_{x=0}$ and $\theta(x,\tau)|_{x=1} = \theta_s$ respectively. By (7) and the boundary conditions, we can obtain

$$\frac{\mathrm{d}\alpha}{\mathrm{d}\tau} = \frac{\alpha\frac{\mathrm{d}\bar{\theta}}{\mathrm{d}\tau} + Q_b - q_0}{\theta_s - \bar{\theta} + n_e},$$

where $\bar{\theta}(\tau) = \int_0^1 \theta(x,\tau)\mathrm{d}x$. Integrating the above equation on $(\tau, \tau+\Delta\tau)$, we have

$$\alpha(\tau+\Delta\tau) - \alpha(\tau) = \frac{1}{\theta_s - \bar{\theta} + n_e}\left\{\alpha[\bar{\theta}(\tau+\Delta\tau) - \bar{\theta}(\tau)] + \int_\tau^{\tau+\Delta\tau}(Q_b - q_0)\mathrm{d}\tau\right\}.$$

Let $H_E^1(\Omega) = \{v \in H^1(\Omega), v(1) = 0\}$, where Ω is the interval $[0, 1]$ and $H^1(\Omega)$ is a Sobolev space. The equivalent variational form of (7) can be written as

$$\left(\frac{\partial\theta}{\partial\tau}, \phi\right) + \left(\frac{D(\theta)}{\alpha^2}\theta_x, \phi_x\right) = -\left(\frac{K(\theta)}{\alpha} - \frac{D(\theta)}{\alpha^2}\theta_x\right)\phi\Big|_0^1 + \int_0^1 \frac{K(\theta)}{\alpha}\phi_x\mathrm{d}x + \frac{\dot{\alpha}}{\alpha}x\phi\theta\Big|_0^1 - \int_0^1 \frac{\dot{\alpha}}{\alpha}x\theta\phi_x\mathrm{d}x - \int_0^1 \frac{\dot{\alpha}}{\alpha}\theta\phi\mathrm{d}x, \tag{8}$$

where $(\cdot,\cdot)$ is the inner product in $L^2(\Omega)$ space.

Divide $[0, 1]$ into n parts, so there are $n+1$ grid points: $0 = x_1 < x_2 < \cdots < x_{n+1} = 1$, where x_1 and x_{n+1} are the boundary points. Denote $e_i = (x_i, x_{i+1})$, $i = 1, \cdots, n$ for n subdomains. Define a finite element space $V_h \subset H_E^1(\Omega)$ such that $V_h = \{v_h \in C[0,1],\ v_h|e_i$ is a linear function, $1 \leqslant i \leqslant n$, and $v_h(1) = 0\}$. Let $\{\phi_i\} \subset V_h$ be the finite element basic functions $\phi_i(x_j) = \delta_{ij}(i, j = 1, \cdots, n)$. Then θ can be written as follows:

$$\theta(x,\tau) = \sum_{i=1}^n X_i(\tau)\phi_i(x) + \theta_s.$$

By the expression of θ and (8), we can obtain the semi-discrete equations:

$$\begin{cases}[A]\{X\} + [B]\left\{\frac{\mathrm{d}X}{\mathrm{d}\tau}\right\} = \{F\},\\ \{X(0)\} = (\theta_0(x_1) - \theta_s, \cdots, \theta_0(x_n) - \theta_s)^{\mathrm{T}},\end{cases} \tag{9}$$

where

$$\begin{cases}[A] = [A_{ij}],\\ A_{ij} = \int_0^1\left[\frac{D(\theta)}{\alpha^2}\frac{\mathrm{d}\phi_i}{\mathrm{d}x}\frac{\mathrm{d}\phi_j}{\mathrm{d}x} + \frac{\dot{\alpha}}{\alpha}\phi_i\phi_j\right]\mathrm{d}x,\\ [B] = [B_{ij}], B_{ij} = \int_0^1\phi_i\phi_j\mathrm{d}x,\\ \{F\} = [F_i],\\ F_i = -\left[\frac{K(\theta)}{\alpha} - \frac{D(\theta)}{\alpha^2}\theta_x\right]\phi_i\Big|_0^1 - \frac{\dot{\alpha}}{\alpha}\theta_s\int_0^1\phi_i(x)\mathrm{d}x + \int_0^1\left[\frac{K(\theta)}{\alpha} - \frac{\dot{\alpha}}{\alpha}x\theta\right]\frac{\mathrm{d}\phi_i(x)}{\mathrm{d}x},\\ \{X\} = (X_1(t), \cdots, X_n(t))^{\mathrm{T}},\\ \left\{\frac{\mathrm{d}X}{\mathrm{d}\tau}\right\} = \left(\frac{\mathrm{d}X_1}{\mathrm{d}\tau}, \cdots, \frac{\mathrm{d}X_n}{\mathrm{d}\tau}\right)^{\mathrm{T}},\\ i, j = 1, \cdots, n,\end{cases}$$

and θ_0 is the initial condition after the coordinate transforming.

To slove the nonlinear ordinary differential equation (9), the time discrete scheme is

$$\begin{cases}\left\{\frac{\mathrm{d}X}{\mathrm{d}\tau}\right\} \approx \frac{\{X\}^{\tau+\Delta\tau} - \{X\}^\tau}{\Delta\tau},\\ \{X\}^{\tau+\Delta\tau/2} \approx \omega\{X\}^{\tau+\Delta\tau} + (1-\omega)\{X\}^\tau,\end{cases} \tag{10}$$

where $\Delta\tau$ is the time step and ω the weighting coefficient, $0 \leqslant \omega \leqslant 1$. The coefficients in Eq. (9) take the values of time $(\tau + \Delta\tau/2)$. According to the time discrete scheme (10), the full discrete scheme can be written as

$$[A]^{\tau+\Delta\tau/2}(\omega\{X\}^{\tau+\Delta\tau} + (1-\omega)\{X\}^{\tau}) + [B]^{\tau+\Delta\tau/2}\frac{\{X\}^{\tau+\Delta\tau} - \{X\}^{\tau}}{\Delta\tau} = \{F\}^{\tau+\Delta\tau/2},$$

then we have

$$[P]^{\tau+\Delta\tau/2}\{X\}^{\tau+\Delta\tau} = [Q]^{\tau+\Delta\tau/2}\{X\}^{\tau} + \{F\}^{\tau+\Delta\tau/2}, \quad (11)$$

where $[P] = \omega[A] + \frac{1}{\Delta\tau}[B]$ and $[Q] = (\omega-1)[A] + \frac{1}{\Delta\tau}[B]$. Since the mass-lumped finite element method is used in computation, and all elements in each row are summed up into the main-diagonal element, oscillatory non-physical profiles are evaded. When $\omega = 1$, an implicit-in-time finite-difference scheme results, even through the various coefficients are evaluated at the half-time level. When $\omega = 1/2$, on the other hand, a time-centered, Crank-Nicolson type algorithm is obtained. To be able to solve $\{X\}^{\tau+\Delta\tau}$ from $\{X\}^{\tau}$, one needs the estimates of the coefficients K and D and then the coefficient matrices $[\boldsymbol{A}]$, $[\boldsymbol{B}]$, $[\boldsymbol{F}]$ and $[\boldsymbol{P}]$, $[\boldsymbol{Q}]$ at the half-time level $\tau + \Delta\tau/2$. We take an iterative method to solve the problem:

Step 1. $\{X\}^{\tau+\Delta\tau/2}$ is obtained through a linear extrapolation from $\{X\}^{\tau-\Delta\tau}$ and $\{X\}^{\tau}$. If $\tau = 0$, then $\{X\}^{\tau+\Delta\tau/2}$ equals $\{X\}^{\tau}$.

Step 2. Solve $\{X\}^{\tau+\Delta\tau}$ by $\{X\}^{\tau}$ and $\{X\}^{\tau+\Delta\tau/2}$.

Step 3. Use $\{X\}^{\tau+\Delta\tau/2} = \frac{1}{2}(\{X\}^{\tau} + \{X\}^{\tau+\Delta\tau})$ to get the next $\{X\}^{\tau+\Delta\tau/2}$.

Step 4. Use $\{X\}^{\tau}$ and the new $\{X\}^{\tau+\Delta\tau/2}$ to get the next $\{X\}^{\tau+\Delta\tau}$.

Step 5. Repeat Step 3 and Step 4 until the difference of the two neighboring $\{X\}^{\tau+\Delta\tau}$ is less than a given value.

2 Coupling of the soil moisture model with the VIC model

Liang et al. described the VIC model in [4] and [5] in detail. The VIC model is a macroscale hydrologic model which is based on the energy and water balance equations and can be run on grid cells. The macroscale here denotes the critical scale described by subgrid spatial variability by means of statistics (Wood et al.[20]). The VIC model has been used successfully on long rivers (for example, Abdulla et al.[21], Lohmann et al.[22], Nijssen et al.[23], and Wood et al.[24]). VIC calculates the vertical energy and water fluxes based on the soil properties and vegetation types on grid cells, which include subgrid spatial variability of infiltration capacity and precipitation, and vegetation types within a grid cell. The drainage between neighboring soil layers is presented dynamically and the unsaturated moisture conductivity is the power function of soil moisture[14]. The base flow follows the Arno model conceptualization, which is applied only to the lowest soil layer. In order to calculate the subgrid variability of infiltration, the VIC model adopts the method of the Xinanjiang model[25]. In this method, the acquirable infiltration capacity described by a spatial probability distribution is used as a function of the fraction of the saturated area. The excessive precipitation directly forms the surface runoff. Every soil column is divided into three layers and the depth of these layers is given in the model.

At each time step, the VIC model first calculates the surface fluxes based on the three layers, which are used as the infiltration condition of the soil moisture model. Secondly, the soil moisture model is called to calculate the moisture and the water table on the fine grid system of the soil moisture model itself and redistributes the moisture on the fine grid to the three layers. And then the base flow, evaporation, and energy budget are solved on the three layers. At the next time step, the initial condition of the soil moisture model takes the moisture values on the fine grid, instead of the three layers, calculated by the last time step.

3 Numerical simulations

In this section, groundwater tables simulated with the soil moisture model and the coupling of the soil moisture model with the VIC model are compared with the observational data. We take the groundwater table of the monitoring well as the observational data and the data of the meteorological station near the well as the forcing data. Two kinds of numerical tests are considered: (1) Based on the precipitation, the maximum and the minimum temperatures, the runoff (surface runoff and base flow) and evaporation are calculated by the VIC model whose surface runoff mechanism has been improved, and further the infiltration is obtained. Taking the infiltration as the upper boundary condition, we can simulate the groundwater table with the new soil moisture model and then compare it with the observational data. (2) The new soil moisture model coupled with the VIC model is run to simulate the groundwater table with the forcing data of the meteorological station and the initial condition of the observational data.

For the two types of simulation, let the positive direction be downward and the origin of coordinates be at the land surface. Map the part between the land surface and the water table to the interval [0, 1], and then divide the interval into n layers evenly, so the spatial step of the soil moisture model is $1/n$, and the time step is $\Delta t = 24$ h.

The water tables of USGS monitoring wells AG700 in Allegheny County and LB372 in Lebanon County of Pennsylvania are taken as the observational data. The meteorological data nearby these two wells are the forcing data. The location of well AG700 is 40°37′34″N 80°06′30″W, the diameter is 15 cm, and the depth is 30.5 m. The location of well LB372 is 40°22′07″N 76°18′08″W, the diameter is 15.24 cm, and the depth is 24.4 m. The meteorological station nearby well AG700 is Bigleverville Station in Allegheny County, and its cooperative ID is 366993. The coordinates of Bigleverville Station are 40°30′N 80°14′W and it belongs to the Lower Allegheny River basin. The meteorological station nearby well LB372 is Lebanon 2 w Station in Lebanon County. Its cooperative ID is 364896 and coordinates are 40°20′N 76°28′W. The data of the groundwater table is provided by USGS and the meteorological data is provided by NCDC. We denote the initial water table as $Deep_0$ and the residual moisture as θ_r (refer to Table 1).

Table 1. Soil parameters and initial conditions corresponding to monitoring wells

Well	$Deep_0$(m)	Initial $\bar{\theta}$	θ_s	K_s/cm·s^{-1}	$-\Psi_s$/cm	b	θ_r
AG700	2.48	0.25	0.476	3.47E-2	21.8	4.90	0.041
LB372	3.35	0.02	0.476	2.91E-3	20.0	5.33	0.02

3.1 Simulation of the soil moisture model (offline simulation)

For the well AG700, the surface runoff, infiltration, and the base flow are obtained by the VIC model with the meteorological data (1 September 1991 ~ 30 September 1998). Then the groundwater table is simulated by the new soil moisture model with the VIC model output. The initial depth of the water table is 2.48 m and the unsaturated area is divided into 20 layers after the coordinate transform. Fig. 1(a) gives the daily precipitation series. The "offline" curve vs. the "observation" curve in Fig. 1(b) shows the comparison of the groundwater table between the offline test and the observational data.

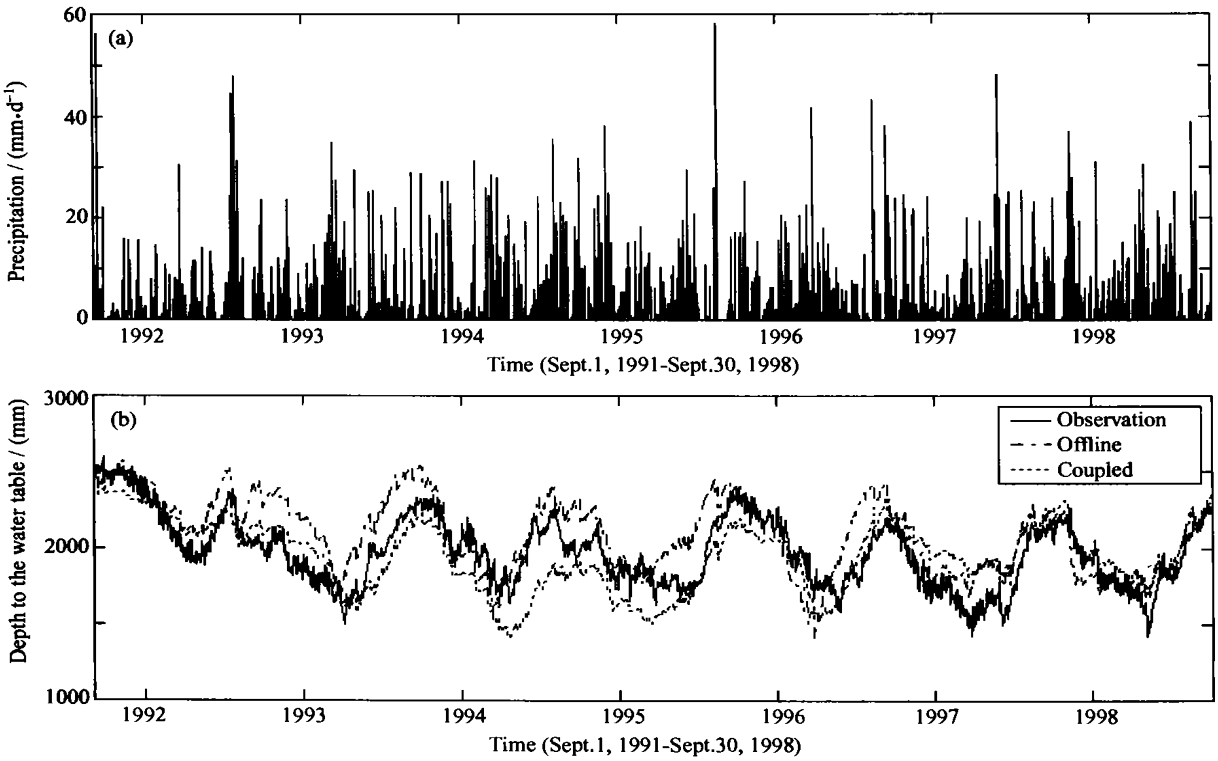

Fig. 1. Comparison of the water table of well AG700 between the simulation results and the observational data. (a) Precipitation series; (b) comparison of the water tables.

3.2 Simulation of the soil moisture model coupled with the VIC model

Using the coupled model (soil moisture model coupled with the VIC model), the groundwater table is simulated with the meteorological data and the initial observational data under the same grid system as the offline test, and is compared with the observational data. In Fig. 1(b), the "coupled" curve vs. the "observation" curve shows the comparison of the groundwater table between the coupled simulation and the observational data. From the figure, it is shown that the observed groundwater table is simulated quite well by the coupled model and the three curves coincide generally to a great extent.

For the well LB372, the surface runoff, infiltration, and the base flow are obtained by the VIC model with the meteorological data (1 October 1991 ~ 30 December 1998). Then the new soil moisture model is called to simulate the groundwater table and the soil moisture. The initial depth of the water table is 3.35 m and the unsaturated area is again divided into 20 layers. Fig. 2(a) gives the daily precipitation series. Fig. 2(b) shows the comparison of the groundwater table between the coupled test and the observational data. From Figs. 1 and 2, it is shown that the soil moisture model can capture the groundwater table dynamically to a great extent.

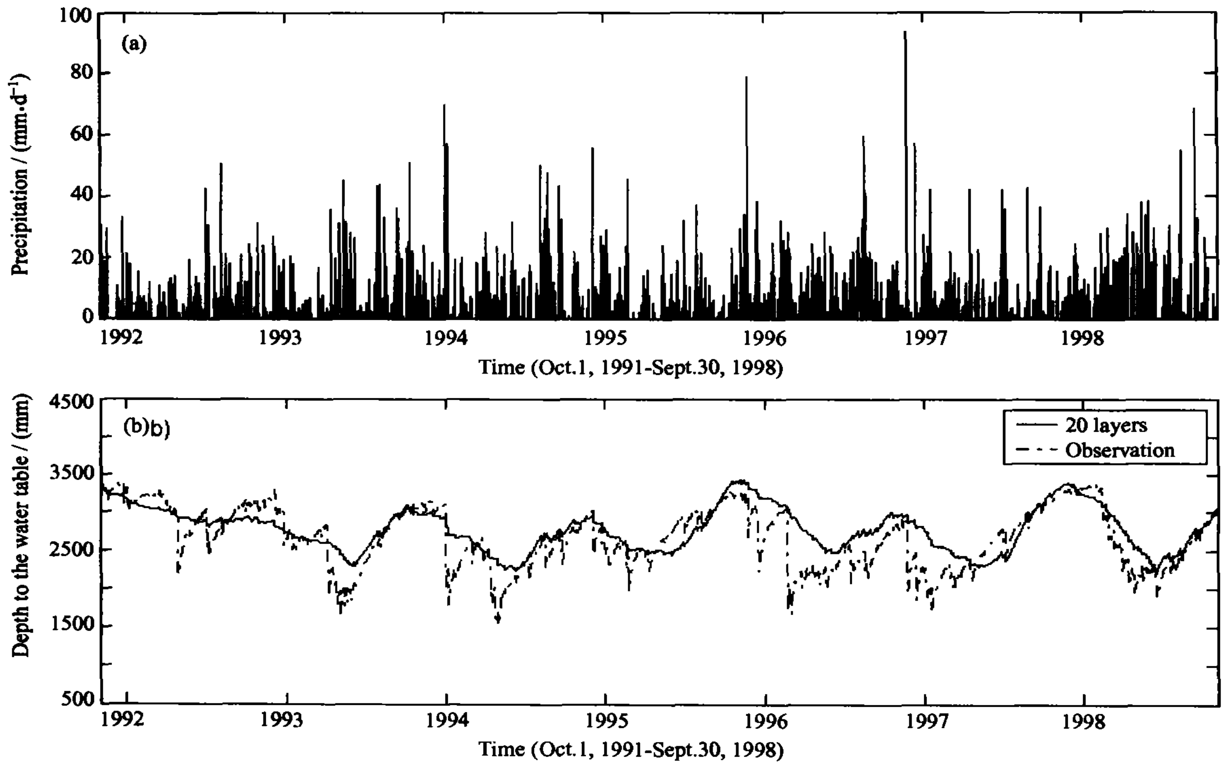

Fig. 2. Comparison of the water table of well LB372 between the simulation result and the observational data. (a) Precipitation series; (b) comparison of the water tables.

4 Conclusion

In land-atmospheric interactions, the dynamic variation of the groundwater table can be described as a moving boundary problem. In this paper, the moving boundary problem is reduced to a fixed boundary problem by coordinate transformation. A new model for simulating groundwater table is developed using the mass-lumped finite element method. With this method, discretization is needed only in the unsaturated area, and with about 20 grid points, a high resolution result can be obtained, and the computational cost is decreased. Two kinds of tests (offline test and coupled test) show that the simulation results coincide with the observational data generally to a great extent. This study is significant since it captures the general nonlinear interaction of the climate system, improves the understanding of the interaction between groundwater and soil moisture, and researches the impacts of climate changes on groundwater.

References

1 Pan, J. Z. et al. The Reasonable Configuration of Water Resource in the North of China and the Problem of Moving Water From South To North. Beijing: Publishing Company of Water Conservancy and Hydroelectricity of China, 2001, 3.

2 Zhao, W. Z. et al. Review of several problems on the study of eco-hydrological processes in arid zones. Chinese Science Bulletin (in Chinese), 2002, 47(5): 353.

3 Dai, Y. J. et al. A land surface model (IAP94) for climate studies, I: Formulation and validation in off-line experiments. Advances in Atmospheric Sciences, 1997, 14: 443.

4 Liang, X. et al. A simple hydrologically based model of land surface water and energy fluxes for general circulation models. Journal of Geophysical Research, 1994, 99(7): 14415.

5 Liang, X. et al. A one-dimensional statistical dynamic representation of subgrid spatial variability of precipitation in the two-layer variable infiltration capacity model. Journal of Geophysical Research, 1996, 101(D16): 21403.

6 Liang, X. et al. A new surface runoff parameterization with subgrid-scale soil heterogeneity for land surface models. Advances in Water Resources, 2001, 24(9~10): 1173.

7 Chow, V. T. et al. Applied Hydrology. New York: McGraw-Hill, 1988, 572.

8 Dirmeyer, P. A. et al. The pilot phase of the global soil wetness project: A pilot project for global land surface modeling and validation. Bull. Amer. Meteor. Soc., 1999, 80: 851.

9 Dingman, S. L. Physical Hydrology. Engelwood Cliff: Prentice Hall, 1994, 575.

10 Xue, Y. K. et al. A simplified biosphere model for global climate studies. J. Climate, 1991, 4: 345.

11 Liang, X. et al. Surface soil moisture parameterization of the VIC-2L model: Evaluation and modifications. Global and Planetary Change, 1996, 13: 195.

12 Liang, X. et al. The project for intercomparison of land-surface parameterization schemes (PILPS) phase-2c Red-Arkansas River basin experiment: II. Spatial and temporal analysis of energy fluxes. Global and Planetary Change (special issue), 1998, 19(1~4): 137.

13 Furzeland, R. M. A comparative study of numerical methods for moving boundary problems. J. Int. Maths. Appl., 1980, 20: 411.

14 Campbell, G. S. A simple method for determining unsaturated conductivity from moisture retention data. Soil Sci., 1974, 117: 311.

15 Clapp, R. B. et al. Empirical equations for soil hydraulic properties. Water Resour. Res., 1978, 14: 601.

16 Bear, J. Dynamics of Fluids in Porous Media. New York: Dover Pub. Inc., 1972, 764.

17 Xie, Z. H. et al. Numerical simulation of the unsaturated flow equation. Sciences in China (Ser. D) (in Chinese), 1998, 4(14): 429.

18 Xie, Z. H. et al. Numerical simulation of the soil moisture and the flux in the unsaturated flow. Progress in Natural Science (in Chinese), 1999, 4(12): 1280.

19 Xie, Z. H. et al. An unsaturated soil flow problem and its numerical simulation. Advances in Atmospheric Sciences, 1999, 16(2): 183.

20 Wood, E. F. et al. Effects of spatial variability and scale with implications to hydrologic modeling. J. Hydrol., 1988, 102: 29.

21 Abdulla, F. A. et al. Application of a macroscale hydrologic model to estimate the water balance of the Arkansas-Red River basin. J. Geophys. Res., 1996, 101(D3): 7449.

22 Lohmann, D. et al. Regional scale hydrology II. Application of the VIC-2L model to the Weser River. Hydrological Sciences Journal, 1998, 43(1): 143.

23 Nijssen, B. et al. Streamflow simulation for continental-scale river basins. Water Resour. Res., 1997, 33(4): 711.

24 Wood, F. et al. Hydrological modeling of continental-scale basins. Annual Review of Earth and Planetary Sciences, 1997, 25: 279.

25 Zhao, R. J. et al. The Xinanjiang model. In: Hydrological Forecasting Proceedings Oxford Symposium. IAHS 129, 1980, 351.